

Satellite number density profiles of primary galaxies in the 2dFGRS.

Laura Sales, and Diego G. Lambas

*Grupo IATE, Observatorio Astronómico de la Universidad Nacional de Córdoba, Argentina.
Consejo Nacional de Investigaciones Científicas y Técnicas.*

1 October 2018

ABSTRACT

We analyse the projected radial distribution of satellites around bright primary galaxies in the 2dFGRS. We have considered several primary-satellite subsamples to search for dependences of the satellite number density profiles, $\rho(r_p)$, on properties of satellites and primaries. We find significant differences of the behaviour of $\rho(r_p)$ depending on primary characteristics. In star-forming primaries, the satellite number density profile is consistent with power laws within projected distance $20 < r_p < 500$ kpc. On the other hand, passively star-forming primaries show flat $\rho(r_p)$ for $20 < r_p \leq 70$ kpc, well fitted by generalized King models with a large core radius parameter ($r_c \sim 68$ kpc). In the external regions of the haloes ($r_p > 100$ kpc), the density profiles of all primaries are well described by power laws $\rho(r_p) \propto r^\alpha$, although we notice that for red, early spectral type primaries, the outer slope obtained is steeper ($\alpha^{red} \sim 1.12$) than that corresponding to blue, late spectral type primaries ($\alpha^{blue} \sim -0.79$). We have tested our results by control samples of galaxies identical to the samples of satellites in apparent magnitude and projected distance to the primary, but with a large relative velocity. This sample of unphysical primary-galaxy pairs shows a flat radial density profile beyond $r_p = 20$ kpc indicating that our results are not biased toward a decrease of the true number of objects due to catalogue selection effects. Our results can be understood in terms of dynamical friction and tidal stripping on satellites in the primary haloes. These processes can effectively transfer energy to the dark matter, flattening the central steep profiles of the satellite distribution in evolved systems.

Key words: galaxies: haloes - galaxies: formation - galaxies: evolution.

1 INTRODUCTION

In hierarchical models of structure formation, galaxies are mainly the result of the assembling of several small sub-clumps of mass, that merge to each other into larger structures. Nevertheless, there are also several low mass sub-clumps which have survived this process, and at present time, they have turned into satellite galaxies of the main host, the primary galaxy. Thus, the radial distribution of the surrounding mass, $\rho(r)$, can provide useful information to test current models of formation and evolution of structure.

Several analytic expressions for mass density profiles have been proposed in the literature. Earlier on 1972, Gunn & Gott proposed the secondary infall model to explain the formation of objects by a continuous accretion process. The model assumes an Einstein-de Sitter universe, where pressureless and non-interacting dust particles are accreted onto an isolated massive center. This model predicts density pro-

files that follow a power-law shape $\rho(r) \propto r^{-9/4}$. Numerical simulations of the formation and non linear evolution of galaxies, follow mass particles from initial conditions up to their present day configuration allowing for a detail understanding of halo structures. The Cold Dark Matter (CDM) hierarchical scenario have proved to be in agreement with many cosmological observations, and has become the most widely adopted model for structure formation. Within this CDM scenario, a universal law was proposed by Navarro, Frenk & White (1996 and 1997, NFW profile hereafter) from their studies of dark matter haloes. The authors find a simple law that does not depend on either the halo mass nor the spectrum of initial density fluctuations and cosmological model parameters. The NFW profile can be written as $\rho(r) \propto c/(x(1+x)^2)$, where x is the distance r normalized to the radius that contains 200 times the critical density of the Universe (r_{200}), $x = r/r_{200}$. All the variables in this formula are related to the concentration parameter, c , which depends on the mass of the haloes. Massive objects are char-

acterised by lower c values than the low mass systems, so that small haloes are usually more concentrated. Therefore, NFW dark matter haloes have a cuspy inner density profile with $\rho(r) \propto r^{-1}$, while in the outskirts, the density falls as $\rho(r) \propto r^{-3}$. This steep behaviour of $\rho(r)$ at small distances has been confirmed by other authors (Moore et al. 1998, Klypin et al. 2001) who find inner slopes of up to $\rho \propto r^{-1.5}$.

Observationally, at galactic scales the flat behaviour of external HI rotational curves indicates a linear growth of mass with galactocentric distance, suggesting an isothermal density profile, $\rho(r) \propto r^{-2}$. On the other hand, several authors found cores instead of cuspy behaviour at the central regions of galaxy haloes (Salucci & Burkert 2000, de Blok et al. 2001, Gentile et al. 2004). CDM models are unlikely to reproduce such constant density profiles obtained from observational data in the center of haloes, so alternative dark matter candidates have been proposed to reconcile theoretical predictions with observations (see for instance Spergel & Steinhardt 2000). Nevertheless, there are some attempts to reproduce central galaxy cores in numerical simulations within universe models dominated by cold dark matter. El-Zant et al. (2001) focus their study on the effects of dynamical friction on density profiles of galaxies, showing that it is possible to obtain a final core feature in haloes starting from a NFW cuspy initial density profile. Within the CDM scenario, the authors explore the energy transport from baryonic clumps to the dark matter component, which heats up the dark matter particles and flattens the density profiles of haloes in their internal regions.

The available observational data used to determine density profiles of galactic haloes does not extend much beyond than the optical radius, since HI rotation curves, are well measured up to $r_p \sim 60 - 100$ kpc in brightest galaxies. At $r_p > 100$ kpc, satellite galaxies represent an interesting alternative to constrain density profiles of primary haloes starting from observations. It is not obvious that satellites follow the mass distribution within the parent halos and actually, many simulation results indicates that the density profiles traced by mass particles are steeper than that obtained using subhaloes. Nevertheless, it is important to note that although dark subhaloes are poor mass tracers, galaxies may follow the mass distribution more accurately. Astrophysical processes such as feedback, cooling or tidal disruption may help to explain the differences between the density profiles obtained by subhaloes and particles. Dekel et al. 2002 have proposed that feedback processes are suitable mechanisms for lowering satellite densities. A satellite with smaller density could be easily disrupted before being accreted onto the inner regions of the haloes, preventing the steepening of ρ at small r . Also, Ghigna et al. 2001 using dissipationless high resolution numerical simulations showed that, as a result of tidal disruption and mergers in cluster cores, subhaloes have an anti-biased number density profile with respect to the dark matter in the central regions of the host haloes. Similar results were obtained by Gao et al. (2004). The authors implemented a semi-analytical model in high resolution simulations of cluster haloes finding, particularly in the inner regions, a biased distribution of dark matter subhaloes compared to the dark matter particle distribution. On the other hand, the authors obtain that the radial distribution of galaxies within simulated clusters is closely related to that of the dark matter. In a recent work,

Nagai & Kravtsov (2004) also conclude that galaxies in clusters are expected to give a less biased tracer of the dark matter compared to dark subhaloes. Using high-resolution numerical simulations of galaxy clusters in Λ CDM cosmology and an implementation of a hydrodynamical model for galaxy formation, the authors find a distribution of subhaloes shallower than that of the dark matter particles, in agreement with previous results. However, since tidal disruption is stronger at the outer regions of subhaloes, their baryonic contents are expected to be less affected by tidal effects implying that galaxies are better tracers of the dark matter profile.

Satellite galaxies are used here in an attempt to put constraints on the radial density profiles of primary galaxies. Our work has the aim of studying the projected number density profiles of satellites around isolated primary galaxies up to 500 kpc in the 2dFGRS. We have searched for dependences of density profiles on several primary and satellite properties and we have tested the results using suitable control samples. In section 2 we describe the selection criteria adopted to construct the samples studied, and in section 3 we show the main results obtained. Finally, in Section 4 we discuss and summarise our principal conclusions.

2 PRIMARY AND SATELLITE SAMPLES

This work is based on the 2dF final data release (Colless et al. 2001). This survey contains almost 246000 objects, mainly galaxies; which have been selected from the APM galaxy catalogue. The objects are distributed covering approximately 1500 square degrees of sky in *North* and *South Galactic Cap* strips as well as some random fields. It provides photometric and spectroscopic information, such as positions, redshifts, accurate b_j , B and R SuperCosmos magnitudes, and a spectral classification through the spectral parameter η .

We have selected two galaxy samples, one corresponding to primary galaxies and the other to their associated satellites. The selection criteria applied to primaries can be summarised in a number of conditions over the redshift, luminosity and environment of the candidate galaxies. All our primaries have been restricted to redshifts $0.01 < z < 0.1$ which assures a high level of completeness in the catalogue and the lack of corrections to the Hubble law as distance estimator. These primaries are brighter than $M < -18$ in the absolute blue magnitude B_j . Throughout this paper we assume a Hubble constant $H_0 = 100 \text{ Km/s Mpc}^{-1}$. In order to construct a sample with a suitable isolation criteria for primary candidates we require that any neighbour galaxy within a region of 700 kpc in projected separation and $|\Delta V| \leq 1000$ km/s (where $|\Delta V|$ is the line-of-sight velocity difference) must be at least 1 magnitude fainter than the primary candidate ($B_j^{neigh} - B_j^{prim} > 1$). By doing so, we significantly reduce the possibility of including a single satellite with more than one primary. We have not imposed any further restriction on the morphological types of the primaries since we aim to explore possible dependences of satellite properties on the associated primary.

Concerning the sample of satellites, we have considered objects within projected separations of 500 kpc of any given primary, and within the range $|\Delta V| < 500$ Km/s. Satellite

candidates should be at least two magnitudes fainter than the primary, and additionally they should be objects fainter than $B_j = -18.5$. The conditions applied here are similar to those in previous works and, in our case, they provide a large number of objects suitable for statistical studies.

We have applied a final (conservative) restriction to this sample with the aim of removing group-like systems, then we keep only those primary-satellite systems with up to 4 satellites per central galaxy.

With the criteria described above, the final sample of isolated primary has 1766 objects and the satellite sample is composed by 2590 galaxies.

3 ANALYSIS

At large galactocentric distances, i.e. at more than two optical galactic radii, satellites can provide important information about the dark halo properties. There are several works in the literature based on this assumption (see for instance Zaritsky et al. 1993 and 1997, Mc Kay et al. 2002, Prada et al. 2003). The authors apply a statistical approach to the problem since primary galaxies outside the Local Group, have a low number of detected satellites per galaxy (in our sample the average value of satellites per primary is ~ 1.7). Then, the general procedure adopted is to compose a characteristic primary halo by considering all satellites as belonging to one typical primary.

In our work we adopt this treatment of the data, building several ensembles of satellites corresponding to primaries with different characteristics (luminosity, color index and spectral type) in order to explore the density profile of luminous matter in the outer regions of haloes (up to 500 kpc) as well as possible dependencies on primary and satellite properties.

We have computed the mean projected satellite number density profile, $\rho(r_p)$, for the different samples by counting the number of satellites in bins of projected galactocentric distance r_p , and normalizing to the total number of primaries in each sample. Several profiles for the baryonic component have been proposed in the literature, with and without a central core. In our analysis, we have adopted two theoretical profile fits for the observed number densities. The generalized King profile (King, 1962) which takes the form

$$\rho(r_p) = \sigma_0 \left(\frac{1}{1 + \left(\frac{r_p}{r_c} \right)^2} \right)^\beta$$

where σ_0 is a parameter that fixes the amplitude and the shape of the profile is determined by the core radius r_c and the β parameter. This profile was originally aimed to fit the distribution of stars in globular clusters and also provides an accurate fit to the observed radial distribution of galaxies in rich Abell clusters (Adami et al. 1998). Alternatively, we also consider a simple power-law fit $\rho(r_p) = Ar^\alpha$.

Firstly, we have computed the satellite number density profile corresponding to the complete sample of primaries and with no restriction to satellite properties. The results are displayed in figure 1 where we show the generalized King model that best fits the data with parameters $r_c = 28 \pm 8$

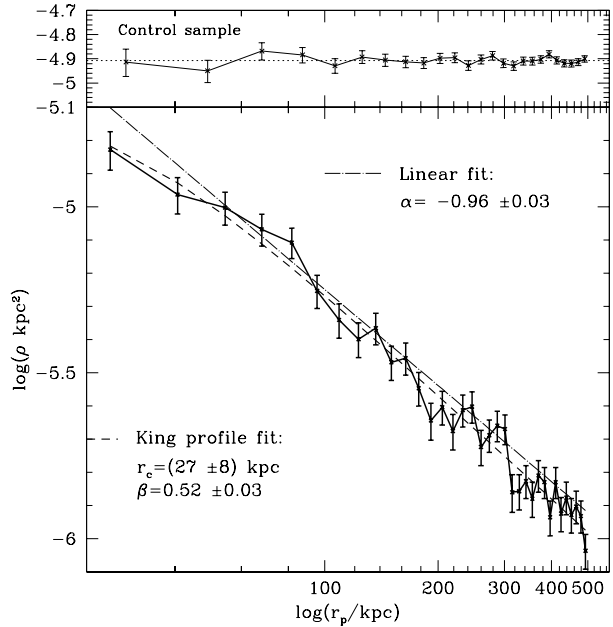


Figure 1. Projected satellite number density profile in the total sample. The short dashed curve indicates the generalized King profile fitted. The best power-law fit is shown in long dashed-pointed line. The upper panel shows in solid curve $\rho(r_p)$ corresponding to the control sample composed by physically unbound galaxies and in dotted line their mean value (see text for details). The error bars are Poisson uncertainties.

kpc and $\beta = 0.52 \pm 0.06$. We also show a power-law fit, $\rho(r_p) \propto r_p^\alpha$ with $\alpha = -0.96 \pm 0.03$ consistent with a projected isothermal halo. The profiles were computed by weighting each data point by its Poisson uncertainty. We have used an implementation of the nonlinear least-squares Marquardt-Levenberg algorithm, and the uncertainty of the parameters were derived from 20 bootstrap re-samplings of the data.

In a recent work, van den Bosch et al. (2004b) analysed the abundance and radial distribution of satellite galaxies in mock galaxy redshift surveys. The authors find a significantly lower number of satellites in 2dFGRS at small separation of primary galaxies compared to the results of the mock catalogues. It is argued that this deficiency could be due to overlap and merging of images corresponding to close projected galaxy pairs in the APM catalogue. We have accounted for this possible bias in our data in the following way: we selected a control sample of projected primary-object systems, namely, pairs of primary-object galaxies that are close only by projection and not in 3-dimensional space. This was accomplished by searching for galaxies inside 500 kpc of projected distance from each isolated primary and at least two magnitudes fainter than it, but with a relative difference velocity $2000 < |\Delta V| < 10000$ km/s. We calculated $\rho(r_p)$ of primaries with these control objects, where we expect the flat profile characteristic of unphysical pair systems in the entire range of projected separations. We found that excluding an inner region of $r_p \sim 20$ kpc, $\rho(r_p)$ for this control sample is flat within errors (see upper panel of fig. 1). With this sample of unbound objects we can obtain a direct measure of how observational effects could affect the determination of the number density profile of isolated

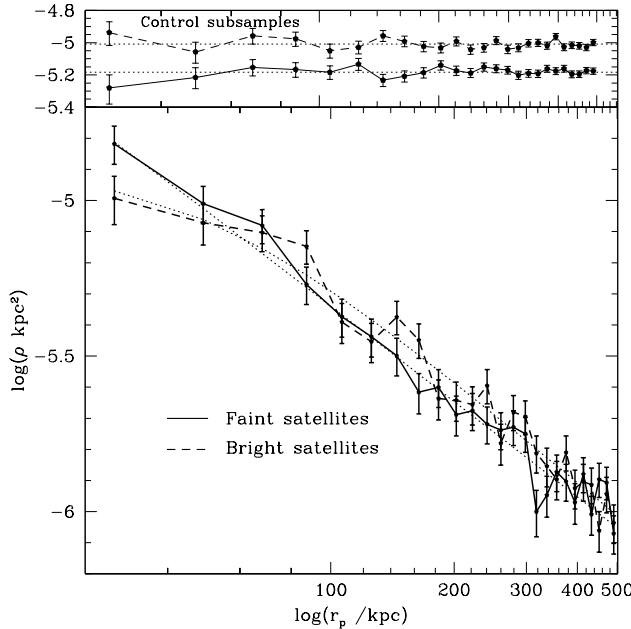


Figure 2. Projected satellite number density profile of faint and bright satellite galaxies (solid and dashed lines respectively). In upper panel we show $\rho(r_p)$ for the equivalent control subsamples. The error bars correspond to Poisson uncertainties.

primary galaxies, since all physical properties (except, by definition, the large relative velocity) of this control sample are comparable to those of the satellites. In particular, we notice that the apparent magnitude distribution of control and satellite samples are very similar, expanding the range $16 < b_j < 19$. The flat behaviour of $\rho(r_p)$ obtained for the unbound primary-object systems provides a very strong argument against a significant lack of pairs due to merge and overlap of images in APM plates and by fiber-fiber collisions in 2dFGRS beyond $r_p = 20$ kpc. Then, according to our selection criteria, the 2dFGRS provide information suitable to trace the number density profiles of primaries in the region $20 \text{ kpc} < r_p < 500 \text{ kpc}$ without significant loss of true satellites. The profiles and fitting parameters shown through this paper were calculated within this interval of r_p .

From fig. 1 it is evident that both analytic approximations, King and power-law profiles, fit well the external region of the primary haloes. However, there is a tendency of the power-law fits to overestimate the amplitude of the density profile in the inner region ($r_p < 50$ kpc).

Our sample of satellites is composed of objects spanning a wide range of absolute magnitude, color indexes and spectral types and it is not obvious that the satellite distribution has a radial profile independent of these properties. For instance, an analysis of numerical simulations of Taylor et al. (2003) suggests that in galactic haloes, low-mass clumps can be found at smaller distances to the center than the most massive ones. Therefore, we may expect to find a difference in the slope of the profile traced by bright or faint satellites, in particular at small separations from the primary.

In order to explore this possibility, we have divided the sample of satellites into bright and faint objects, where the

threshold was taken as the median of the absolute magnitude distribution of satellites. The resulting profiles of bright and faint satellites can be appreciated in figure 2, where solid and dashed lines correspond to faint ($B_j^{sat} > -17.3$) and bright ($B_j^{sat} < -17.3$) satellites respectively. Based on the shape of the total sample $\rho(r_p)$, we have fitted generalized King models to both subsamples (dotted lines).

Consistent with the results from numerical simulations, bright satellites at small projected separations from the primary, $r_p < 50$ kpc, have a flat profile which gradually steepens and becomes consistent with the faint satellite profile beyond $r_p > 100$ kpc. It is clear from this plot that in the external regions of haloes, bright and faint satellites trace the same profile, but that closer to the primary, there is a significant relative excess of faint satellites. This should be reflected in the King profile fitting parameters mainly through the core radius, which is expected to have large values for the bright satellite radial distribution. The resulting parameters are $r_c = 48 \pm 15$ kpc and $\beta = 0.55 \pm 0.04$ for bright satellites, and $r_c = 7 \pm 7$ kpc and $\beta = 0.51 \pm 0.03$ for the faint ones.

We have also explored the dependence of the number density profiles on satellite colour index and spectral type. We have divided the sample of satellites into red and blue objects (taking the median value of the satellite color index distribution as a threshold to divide the samples). We find that red satellites are distributed with a significantly larger core radius compared to the blue ones. Similarly, we divided the sample of satellites taking into account their spectral types. Here, the threshold was taken at $\eta^{sat} = 1.1$ which divides the total sample of satellites into approximately equal number subsamples. We find that the subsample of satellites with a stronger level of star formation activity ($\eta^{sat} > 1.1$) are more frequent at small r_p values than poor star-forming satellites, which show a flatter inner profile.

Nevertheless, the criteria adopted to select the satellite subsamples imply correlations between primary and satellite properties. For example a bright primary is likely to have brighter satellites than a faint primary, and as consequence, color indexes and spectral types of samples of primaries and satellites can be strongly correlated. Therefore it is important to consider the dependence of the profiles on primary properties as well.

Lorrimer et al. (1994) found that primaries of early morphological type tend to have their satellites more centrally clustered than late-type primaries. The authors fitted power-law profiles, $\rho(r_p) \propto r_p^\alpha$, with values of $\alpha \sim -1.0$ and $\alpha \sim -0.8$ for early and late-type primaries respectively. Therefore, we have explored projected satellite number density profiles around primary galaxies with different colour indexes and spectral types (both properties closely related to the morphological type). We have divided the total primary sample into roughly equal number red ($(B_j - R) > 1.11$) and blue ($(B_j - R) < 1.11$) primaries and we compute $\rho(r_p)$ of satellites for both subsamples. For blue primaries, we find the King fitting parameters $r_c = 1 \pm 3$ and $\beta = 0.49 \pm 0.03$. For red primaries the corresponding values are $r_c = 68 \pm 12$ and $\beta = 0.61 \pm 0.06$. These results are in apparent disagreement with Lorrimer et al. since red galaxies (which include more early type morphologies) have a larger core radius. However, as will be discussed later, red primaries have steeper profiles in the outer halo regions.

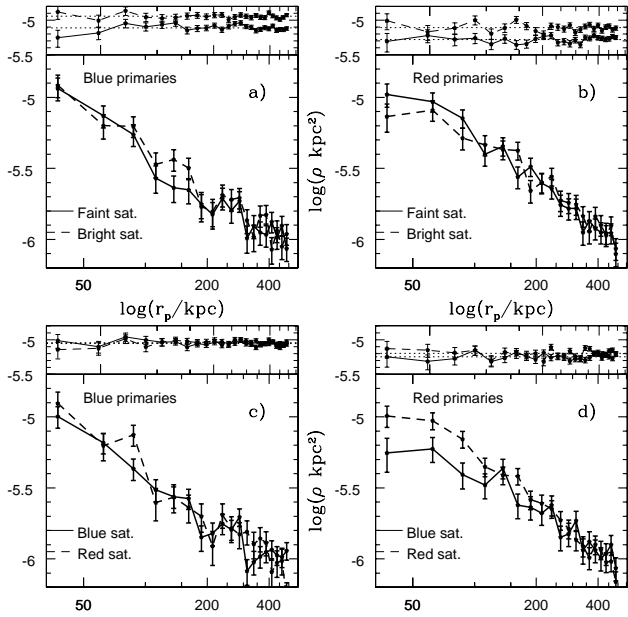


Figure 3. Projected satellite number density profile for blue primaries (both left panels) and red primaries (right panels). The two upper boxes show bright (dashed line) and faint (solid line) satellites. In c) and d) we show in dashed curve the red satellites, and in solid line the blue ones. As before, the results of control subsamples are shown in small panels. The errors correspond to Poisson uncertainties

We notice that since red primaries are brighter (with mean value of $B_j = -20.1$ compared to the corresponding $B_j = -19.6$ of blue primaries) a larger fraction of bright, red associated satellites are expected which would tend to have a large core radius. In order to disentangle the effects of primary and satellite properties on the shape of the profiles we have considered two primary subsamples (red and blue) separately, and we have computed $\rho(r_p)$ for different luminosity and colour of satellites in each subsample of primaries. Thus, the result of this test could provide unambiguous evidence that the profiles depend mainly on primary properties or alternatively on satellite properties. The results of this analysis are shown in figure 3 where the left panels (a) and (c) show profiles corresponding to blue primaries. In the right panels (b) and (d) we show $\rho(r_p)$ for red primaries. We use different lines to distinguish between satellite luminosities (upper panels) and satellite color indexes (bottom panels). By comparing left and right panels we can see that red primary galaxies (right panels) have flat inner density profile, a trend that remains unchanged regardless of colour or luminosity of the satellites. As a consequence, King profile fits of red primaries have a large core radius (~ 68 kpc compared to $r_c \sim 1$ kpc for blue primaries independent of satellite characteristics).

Due to the correlation between spectral type and colour indexes of galaxies, we expect to find differences in density profiles of primaries with different η spectral types. Madgwick et al. (2003) have proposed a classification of galaxies based on Principal Component Analysis through a pa-

Table 1. Parameters of the generalized King density profile fit for different subsamples.

Subsample	r_c	β
Total sample	28 ± 8	0.52 ± 0.03
Red primaries	68 ± 12	0.65 ± 0.06
Blue primaries	1 ± 3	0.48 ± 0.03
$\eta^{prim} < -1.4$	56 ± 12	0.65 ± 0.04
$\eta^{prim} > -1.4$	1 ± 3	0.46 ± 0.03

rameter η . Taking into account this work, we have adopted $\eta = -1.4$ in order to divide the primary sample into two subsamples, type I primaries (objects with $\eta^{prim} < -1.4$) and primaries with a large star formation rate ($\eta^{prim} > -1.4$). The satellite number density profiles obtained are consistent with those of the previous analysis of colour indexes, in the sense that poor star-forming primaries have larger values of r_c and β compared to those of active star-forming primaries. The King parameters that best fit the data are shown in table 1. We also give in this table the results of red and blue primaries and of the total sample of primaries and satellites for a clear comparison.

The flattening of $\rho(r_p)$ in the internal regions of haloes ($20 < r_p < 70$ kpc) would imply a real deficiency of satellites at small r , although a possible bias due to poor detection of satellites near bright primaries should also be considered. Therefore in order to explore further this possibility, we have determined $\rho(r_p)$ for faint and bright subsamples of red and blue primaries. We find that red primaries have larger core radii than blue primaries for both, bright ($B_j < -20.1$) and faint ($B_j > -20.1$) galaxies. The results for the subsample of bright primaries are $r_c^{red} = 71 \pm 15$ and $r_c^{blue} = 8 \pm 5$, while for the faint primary subsample we obtained $r_c^{red} = 53 \pm 12$ and $r_c^{blue} = 1 \pm 5$. Thus, we conclude that primary colour index is a main parameter that characterizes the core radius of the radial distribution of satellites, although most luminous primaries have larger r_c once restricted to a range of colour indexes.

From inspection to figure 3 we can see that the density profile of blue galaxies is well fitted by a power-law at all r_p explored. Red primaries however are characterized by larger values of r_c , and depart significantly from a power-law at small r_p . Nevertheless, in the external regions ($r_p > 70$ kpc) the satellite number density profiles are consistent with a power-law behaviour for all samples. A reliable estimate of the departure of $\rho(r_p)$ from a power-law can be obtained by comparing the expected number of satellites, N_e , from a pure power-law to the number of objects actually found N_{obs} .

We have fixed the parameters A and α of the power-law fits $\rho(r_p) = Ar^\alpha$ for the range of distances $100 < r_p < 500$ kpc, where all the profiles are seen to be well described by power-laws. We have considered the previously defined red and blue, and, $\eta^{prim} < -1.4$ and $\eta^{prim} > -1.4$ primary subsamples and we have used Monte Carlo simulations to build a mock halo with the same number of satellites for each of these subsamples, obeying a power-law consistent with the observed parameters. This procedure was repeated 30 times

Table 2. Expected (from the best power-law fit) and observed number of satellites, N_e and N_{obs} respectively, for $20 < r_p < 70$ kpc.

Subsample	α	N_e	N_{obs}
Red primaries	-1.11 ± 0.07	183	76
Blue primaries	-0.81 ± 0.08	93	109
$\eta^{prim} < -1.4$	-1.13 ± 0.07	202	96
$\eta^{prim} > -1.4$	-0.77 ± 0.08	87	93

for each subsample to deal with statistical uncertainties. As we must take into account the finite size of the primaries, where no satellites are expected, the simulated spherical mock haloes have been generated in three dimensions in the range $20 < r < 500$ kpc. The generalized King model fits to these haloes give small core radius values, $r_c \sim 7 - 23$ kpc. The comparison between N_e and N_{obs} (expected and observed number of satellites respectively) was made within projected distances $20 < r_p < 70$ kpc, where we observe a strong flattening of density profiles and the main results are listed in table 2.

Regarding external regions of haloes ($r_p > 100$ kpc) the values of α for different primary subsamples (shown in the second column of table 2) indicate that also at large projected distances, $\rho(r_p)$ depends strongly on primary properties. Red and $\eta^{prim} < -1.4$ primaries have a statistically significant steeper outer density profiles than blue or $\eta^{prim} > -1.4$ galaxies. The α values of poor and active star-forming primaries differ up to a $\sim 4.5\sigma$ level. We have mentioned earlier that Lorrimer et al. (1994) obtained similar results for their sample of satellites around early and late type primaries, nevertheless, this agreement with Lorrimer et al. work is present only when restricting our analysis to the outer $r_p > 100$ kpc region.

If we consider now the inner regions of primary haloes, table 2 suggests that the size of the core radius of density profiles correlates with the deficiency of satellites near the primary compared to the expected number from power-law fits. Poor star-forming primaries, which are likely to have extended core radii show a large difference between N_e and N_{obs} . On the other hand, consistently with their small core radii, this effect is not present in active star-forming primaries. Moreover, the situation is just the opposite, for blue or $\eta^{prim} > -1.4$ galaxies the number of satellites with small r_p value is larger than the corresponding to the power-law fitted in the external regions.

Therefore, we can consider the core radius as suitable parameter to indicate the scales in which the density profiles of primary galaxies significantly depart from a power-law behaviour. Figure 4 gives a strong support to the latter conclusion, where we have displayed in the left panels the active star-forming galaxies (blue primaries in the upper panel, $\eta^{prim} > -1.4$ galaxies in the bottom), and poor star-forming primaries in the right panels (again, upper and bottom panels contains red and $\eta^{prim} < -1.4$ galaxies respectively). In dashed lines we indicate the power-law density profiles of the corresponding simulated haloes and their dispersion. The vertical line shows the King core radius obtained for each subsample. In the top of all boxes we show $\rho(r_p)$ calcu-

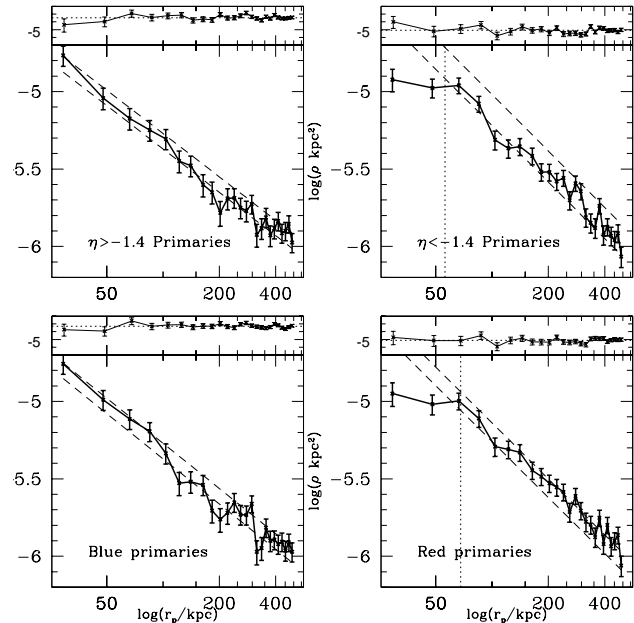


Figure 4. Projected satellite number density profiles for different primary subsamples. Left panels show active star-forming galaxies and the right boxes correspond to poor star-forming primaries. The power-law and its dispersion of simulated haloes are shown in dashed lines. The King core radii calculated are displayed in dotted curve. The test results obtained from control subsamples are also shown in upper small boxes.

lated using control galaxies associated to the same primary galaxies of each subsample. It can be appreciated in the figures that the profiles of control samples show no systematic decrease in the inner regions. We conclude that the flattening of the density profile in the poor star-forming primary subsamples are not likely to be caused by missing satellite images in the source catalogue, but has instead a physical origin.

Although our primary sample satisfies an isolation criteria, poor star-forming galaxies have a higher probability of being in denser regions (probably belonging to groups or larger systems). This fact could increase the loss of faint satellites in primary vicinity due to image overlap and merge. To rule out a bias in the profiles due to differences on the primary environment, we have explored the Σ_5 density parameter for both, red and blue primary subsamples, obtaining a suitable statistical measure of how crowded is the field near each galaxy. We calculated the projected distance from a primary to the fifth bright galaxy ($B_j < -20$) with a relative radial velocity $|\Delta V| < 1000$ km/s and estimate a local projected density for each primary. The distributions of Σ_5 for red and blue primary galaxies are shown in the bottom panel of fig 5, in dashed and solid line respectively. Both distributions are very similar, indicating that our findings are independent of primary environment since interlopers are not likely to be different for the two subsamples.

We notice that due to our primary and satellite selec-

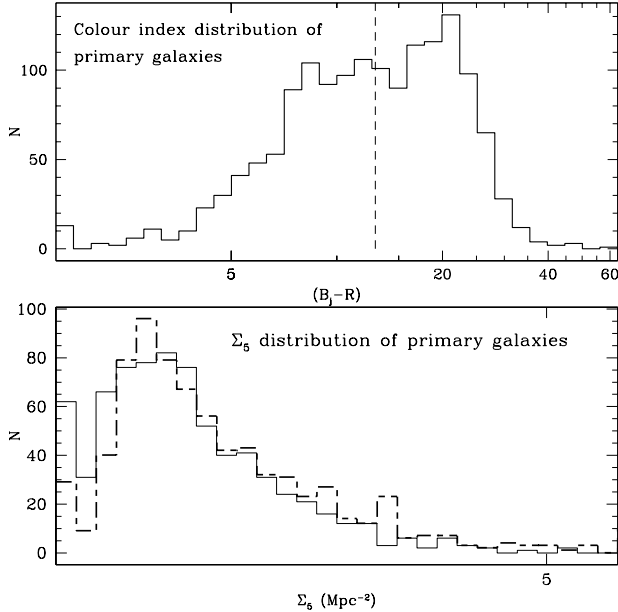


Figure 5. Top box shows the $B_j - R$ colour index distribution of the primary sample. In dashed line we show the threshold used to divide blue ($B_j - R < 1.11$) and red ($B_j - R > 1.11$) galaxies. Bottom box shows the distribution of Σ for these primary subsamples, solid (dashed) line correspond to blue (red) galaxies.

tion criteria, bright primaries have a redshift distribution typically shifted toward higher values than the faint subsample. Simultaneously, because the colour-magnitude relation, faint galaxies tends to have smaller color indexes than bright ones. Therefore, our subsample of blue primaries has smaller z values than the red subsample, which could imply a less efficient detection of satellites near to red primaries. To test this possibility, we have considered a subsample of blue and red primaries with roughly equal z distribution (see small box of fig. 6). The resulting profiles are shown in the main box of fig. 6, where it can be appreciated the similarity with our previous results. The King fitting parameters are also shown in the same figure, and are statistically equivalent to those obtained for the full blue and red primary subsamples (see table 1).

Finally, we have explored for a possible dependence of the density profiles of isolated primary galaxies on radial velocity difference, $|\Delta V|$, and also on the number of satellite per primary.

The distribution of satellite radial velocities relative to the primary, $|\Delta V|$, is strongly correlated to the halo masses (Prada et al. 2003, van den Bosch et al. 2004). The authors find that the observations are consistent with Gaussian distributions with dispersions increasing systematically with primary luminosity. Since primary luminosity and colour are correlated, we also expect correlations of the satellite number density profiles with $|\Delta V|$. In order to explore into more detail the dependence of $\rho(r_p)$ on $|\Delta V|$, we have repeated the previous analysis, but considering satellites of high and low $|\Delta V|$ for our red and blue primary subsamples. The adopted $|\Delta V|$ threshold is 160 km/s, approximately the mean value

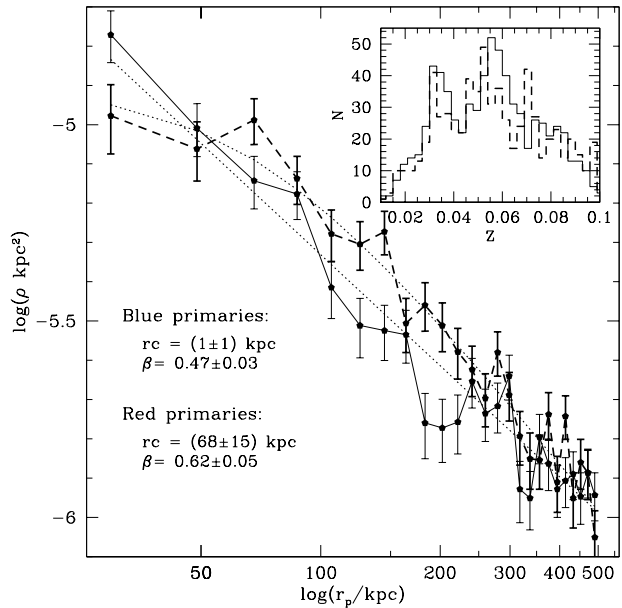


Figure 6. Number of satellites density profiles for blue and red primary subsamples restricted to have a similar redshift distributions. The King profiles fitted are shown in dotted curve. The upper small box shows the corresponding z distributions for both subsamples (solid and dashed line respectively).

of the primary-satellite relative radial velocity distribution. We find that the results previously described do not depend on $|\Delta V|$. In both high and low $|\Delta V|$ subsamples, we find the satellite distribution around red primaries to have a systematically larger core radius than around blue primaries, as obtained before.

Our primary sample contains up to 4 satellites per system and it is interesting to investigate if $\rho(r_p)$ depends on the number of satellites in a system. Thus, we considered two subsamples of primaries, the first with 1 and 2 satellites and the second with 3 and 4. But as before, the resulting profiles for the blue and red primary subsamples does not depend on the number of satellites per system, with red primaries showing flatter profiles than blue ones regardless of the number of satellite per primary considered.

4 SUMMARY

In the hierarchical scenario, the growth of structures is expected to happen from low mass objects to larger structures. In such a picture, the accretion of satellites onto primaries is a common process that may determine many properties of the large galaxies (Klypin et al. 1999, Moore et al. 1999, Abadi et al. 2003, Moore et al. 2003). With the aim of studying the density profile of isolated galaxies up to 500 kpc of projected distance, we have analysed the projected number density profiles of satellites around bright primaries in the 2dFGRS. Although van den Bosch et al. (2004) using mock galaxy redshift surveys claim that 2dFGRS data is unable to put constraints on the radial distribution of satellites around primary galaxies, in our analysis, we have obtained flat density profiles for control subsamples of objects as close in pro-

jection to primaries than real satellites and with the same apparent magnitude distribution but with large relative velocity. This test gives a clear indication that neither image overlap and merging of APM galaxies nor fiber collisions have a significant effect on our analysis of the radial distribution of objects near an isolated primary, and so our results are essentially free of such possible systematics in the range $20 < r_p < 500$ kpc.

For the total sample we find a weak, but still significant, departure from a power law at small galactocentric projected distances ($20 < r_p < 50$ kpc). However, the subsample of star-forming primaries is consistent with a pure power law fit in the range $20 < r_p < 500$ kpc. On the other hand, the satellite radial distribution of poor star-forming primaries is characterized by a flat $\rho(r_p)$ at small r_p consistent with a power law with a constant density core. Accordingly, generalized King profiles with a large core radius parameter ($r_c \sim 70$ kpc) provide good fits to the data. We notice, however, that $\rho(r_p)$ is significantly steeper in the outer regions of these primaries than in blue, late spectral type primaries (we find $\alpha \sim -1.12$ for poor star-forming primaries and $\alpha \sim -0.79$ for galaxies with higher levels of star formation) as it was earlier suggested by Lorrimer et al. 1994. We have also explored dependences of $\rho(r_p)$ on satellite properties finding that the number density profiles of faint, blue, or $\eta > 1.1$ satellite subsamples have smaller core radii and are well fitted by power law fits. By contrast, bright, red, or poor star-forming satellite subsamples require large core radii. Nevertheless, we argue that these dependencies of the number density profiles on satellite properties are probably caused by correlations between primary and satellite properties, since the differences between density profiles of satellites of different types are not present when the subsamples are restricted to belong to primaries of a given colour index and spectral type.

Results from numerical simulations can help to interpret our findings. As pointed out in the Introduction, several authors concluded that the cluster density profiles obtained using the radial distribution of subhaloes are flattened due to tidal disruption effects. Since primary-satellites systems can be considered as a small scale version of clusters, tidal forces can destroy some of the satellites and bias the observed $\rho(r_p)$. As shown by Nagai & Kravstov (2004) results, this tidal disruption is expected to be stronger for subhaloes near the center of the host halo, and as consequence, a lower number of substructures is found at small cluster-centric distances. Even taking into account that tidal mass loss mainly affects outer regions of subhaloes, a percentage of baryonic mass could be lost for each satellite orbiting in the potential well of the primary. After several orbits, a satellite may lose a significant fraction of its stars, falling down to the detection limit of the catalogue, or in a more extreme case, it can be completely disrupted by primary drag forces. In such scenario tidal mechanisms could explain the flattening of the inner number density profile. Nevertheless, our results indicate that only galaxies dominated by old stellar populations (large colour index values and low η -spectral type parameters) have a core feature in their profiles, while for active star-forming primaries $\rho(r_p)$ is consistent with a pure power-law. We can interpret this behaviour as an evolutionary effect, since primaries with a low rate of star formation are probably old systems so that satellites orbiting around

these galaxies may have been exposed to tidal forces during long time periods.

We notice that it remains unclear the validity of considering satellites galaxies as suitable mass tracers. As Nagai & Kravtsov pointed out, there are selection effects that could affect the subhalo and the galaxy radial distribution. Therefore, we can not make conclusive statements on the dark matter distribution around primary galaxies starting from their satellite radial distribution. High resolution numerical simulations with reliable star formation schemes including feedback process may provide consistent models of the distributions of mass and satellites around bright primaries and give a detailed explanation of the observational results.

ACKNOWLEDGMENTS

We thank the Referee for helpful comments and suggestions which greatly improved the previous version of this paper. This work was partially supported by the Consejo Nacional de Investigaciones Científicas y Técnicas, Agencia de Promoción de Ciencia y Tecnología, Fundación Antorchas and Secretaría de Ciencia y Técnica de la Universidad Nacional de Córdoba.

REFERENCES

- Abadi, M.; Navarro, J.; Steinmetz, M.; Eke, V., 2003, ApJ 597, 21.
 Adami, C. et al., 1998, A&A 339, 63
 Colless, M. et al. 2001, MNRAS 328, 1039
 Dekel, A; Devor, J. & Hetzroni, G., 2003, MNRAS 341, 326
 de Blok, W; Mc Gaugh, S. & Rubin, V., 2001, AJ 122, 2396
 Diemand, J.; Moore, B. & Stadel, J., 2004, MNRAS 352, 535
 El-Zant, A; Sholsman, I. & Hoffman, Y., 2001, ApJ 560, 363
 Gao, L. et al., 2004, MNRAS, 352, L1
 Gentile, G. et al., 2004, pre-print astro-ph/0403154
 Ghigna, S. et al., 2001, ApJ 544, 616
 Gunn, J & Gott, J., 1972, ApJ 176, 1
 Klypin, A. et al., 1999, ApJ 522, 82
 Klypin, A. et al., 2001, ApJ 554, 903
 Lorrimer, S. et al., 1994, MNRAS 269, 696
 Madgwick, D. et al., 2003, MNRAS 343, 871
 Mc Kay, T. et al., 2002, ApJ 571, L85
 Moore, B. et al., 1998, ApJ 499, L5
 Moore, B. et al., 1999, ApJ, 524, L19
 Navarro, J.; Frenk, C. & White, S., 1996, ApJ 462, 563
 Navarro, J.; Frenk, C. & White, S., 1997, ApJ 490, 493
 Prada, F. et al., 2003, ApJ 598, 260
 Salucci, P & Burkert, A., 2000, ApJ 537, L9
 Spergel, D. & Steinhardt, P. , 2000, Physical Review Letters 86, 3760
 Taylor, J.; Silk, J & Babul, A., 2003, pre-print astro-ph/0312086
 van den Bosch, F. et al., 2004, pre-print astro-ph/0404033
 van den Bosch, F. et al., 2004b, pre-print astro-ph/0406246
 Zaritsky, D.; Smith, R.; Frenk, C.; White, S., 1993, ApJ, 405, 464.
 Zaritsky, D.; Smith, R.; Frenk, C.; White, S., 1997, ApJ Letters, 478, L53.